FOR THE RECORD

Interaction between the C-terminal domains of measles virus nucleoprotein and phosphoprotein: A tight complex implying one binding site

David Blocquel,[1] Johnny Habchi,[1] Stéphanie Costanzo,[1] Anthony Doizy,[1] Michael Oglesbee,[2] and Sonia Longhi[1]*

[1]CNRS, Aix-Marseille Université, Architecture et Fonction des Macromolécules Biologiques (AFMB) UMR 7257, 13288 Marseille, France

[2]Department of Veterinary Biosciences, Ohio State University, Columbus, Ohio 43210

Received 15 May 2012; Revised 27 June 2012; Accepted 17 July 2012
DOI: 10.1002/pro.2138
Published online 10 August 2012 proteinscience.org

Abstract: The intrinsically disordered C-terminal domain (N_{TAIL}) of the measles virus (MeV) nucleoprotein undergoes α-helical folding upon binding to the C-terminal X domain (XD) of the phosphoprotein. The N_{TAIL} region involved in binding coupled to folding has been mapped to a conserved region (Box2) encompassing residues 489–506. In the previous studies published in this journal, we obtained experimental evidence supporting a K_D for the N_{TAIL}–XD binding reaction in the n*M* range and also showed that an additional N_{TAIL} region (Box3, aa 517–525) plays a role in binding to XD. In striking contrast with these data, studies published in this journal by Kingston and coworkers pointed out a much less stable complex (K_D in the μ*M* range) and supported lack of involvement of Box3 in complex formation. The objective of this study was to critically re-evaluate the role of Box3 in N_{TAIL}–XD binding. Since our previous studies relied on N_{TAIL}-truncated forms possessing an irrelevant Flag sequence appended at their C-terminus, we, herein, generated an N_{TAIL} devoid of Box3 and any additional C-terminal residues, as well as a form encompassing only residues 482–525. We then used isothermal titration calorimetry to characterize the binding reactions between XD and these N_{TAIL} forms. Results effectively argue for the presence of a single XD-binding site located within Box2, in agreement with the results by Kingston *et al.*, while providing clear experimental support for a high-affinity complex. Altogether, the present data provide mechanistic insights into the replicative machinery of MeV and clarify a hitherto highly debated point.

Keywords: isothermal titration calorimetry; intrinsically disordered proteins; folding coupled to binding; entropic penalty; entropic stabilization; paramyxoviruses; nucleoprotein; phosphoprotein

---

David Blocquel and Johnny Habchi contributed equally to the work.

Grant sponsor: Agence Nationale de la Recherche (Physico-Chimie du Vivant); Grant number: ANR-08-PCVI-0020-01. DB is supported by a joint doctoral fellowship from the Direction Générale de l'Armement (DGA) and the CNRS. AD is supported by a doctoral fellowship from the French-Italian University and the Direction Générale de l'Enseignement Supérieur et l'Insertion Professionnelle (DGESIP).

**Correspondence to:* Sonia Longhi, AFMB, UMR 7257 CNRS and Aix-Marseille University, 163, avenue de Luminy, Case 932, 13288 Marseille Cedex 09, France. E-mail: Sonia.Longhi@afmb.univ-mrs.fr

Introduction

Measles virus (MeV) is a member of the *Morbillivirus* genus. It has a nonsegmented, single-stranded, negative sense ribonucleic acid (RNA) genome that is encapsidated by the nucleoprotein (N). This N:RNA complex, rather than naked RNA, is the template for both transcription and replication. The viral polymerase (L) does not directly bind viral genomic RNA during the transcription and genome replication, but, instead, is tethered onto the nucleocapsid template via the viral phosphoprotein (P). The P protein simultaneously binds to L and to the exposed C-terminal disordered domain of N (N_{TAIL}, amino acids 400–525) via its C-terminal X domain (XD, amino acids 459–507).[1–9] Progressive movement of the polymerase along its template is thus thought to require cycles of N_{TAIL}–XD binding and release.[10,11]

N_{TAIL} is an intrinsically disordered domain,[12,13] that is, it exists as a dynamic ensemble of interconverting conformers under physiological conditions of pH and salinity.[14–19] Using computational approaches,[13] an α-helical molecular recognition element (α-MoRE, aa 488–499 of N) has been identified within one (namely Box2, aa 489–506) of three N_{TAIL} regions (referred to as Box1, Box2, and Box3) that are conserved within *Morbillivirus* members[20] [see Fig. 1(A)]. MoREs are short-order prone regions within intrinsically disordered domains that have a propensity to undergo induced folding (i.e., a disorder-to-order transition) upon binding to a partner.[22–25] This α-MoRE is involved in binding to XD, and the N_{TAIL} region encompassing residues 486–502 adopts an α-helical conformation in the bound form.[1–9,13,21] Binding of XD to Box2 also induces a reduction in the conformational flexibility of the downstream Box3 region (aa 517–525).[4,6,8] The reduced flexibility does not arise from the establishment of stable contacts between Box3 and XD,[4] instead being attributed to transient, nonspecific interactions.[7] Support for a role of Box3 in N_{TAIL} binding to XD comes from four independent lines of experimental evidence. First, heteronuclear NMR studies carried out on ^{15}N-labeled N_{TAIL} showed that the addition of XD triggered both α-helical folding of Box2 and a minor, though significant, magnetic perturbation within Box3.[2,7] Second, the low-resolution structural model of the N_{TAIL}–XD complex that was derived using small angle X-ray scattering showed lack of a C-terminal appendage exposed to the solvent, suggesting that beyond Box2, Box3 could also be involved in binding to XD.[2] Third, intrinsic fluorescence spectroscopy studies revealed a dose-dependent impact of XD on the fluorescence of a trp residue inserted within Box3.[2] Incidentally, those studies also allowed estimation of the equilibrium dissociation constant (K_D) that was found to be in the submicromolar range (e.g., ~100 n*M*) and in close agreement with the value determined by either surface plasmon resonance (SPR)[2] or isothermal titration calorimetry (ITC).[26] Finally, those previous SPR studies showed that removal of Box3 results in a strong increase in the K_D, with this latter increasing from 80 n*M* to 12 μ*M*.[2] When SPR experiments were carried out using synthetic peptides mimicking Box2 and Box3, a Box2 peptide (aa 487–507), was found to display an affinity for XD that was similar (K_D = 20 n*M*) to that between XD and N_{TAIL} (K_D = 80 n*M*) consistent with the role of Box2 as the primary binding site.[11] Box3 peptide exhibits an insignificant affinity for XD (K_D of ~1 m*M*),[11] consistent with a role for Box3 only in the context of N_{TAIL} and not in isolation. Therefore, we proposed a model where Box3 and Box2 would be functionally coupled in the binding of N_{TAIL} to XD, with the burying of the hydrophobic side of the α-MoRE at the XD interface providing the primary driving force in the N_{TAIL}–XD interaction, while Box3 would act to further stabilize the bound conformation. In contrast to our model, recent data by the group of Kingston argue for an N_{TAIL}–XD binding mechanism in which Box3 is dispensable. In those studies, the authors used both SPR and ITC to characterize binding reactions between XD and synthetic peptides corresponding to amino acids 477–505 (including Box2) or 477–525 (including both Box2 and Box3) of N, and derived a K_D that was either 7.4 or 15 μ*M*, respectively.[27] Those results argue for a much less tight complex than suggested by our previous studies[2,26] in addition to supporting the lack of involvement of Box3.

The objective of this study was to critically reevaluate the role of Box3 in the N_{TAIL}–XD interaction. As our previous studies[2] made use of a truncated form of N_{TAIL} (hereafter referred to as $N_{TAIL\Delta3\text{-}Flag}$) that was devoid of Box3 but did however possess an irrelevant Flag sequence (DYKDDDDK) appended at its C-terminus that might have confounded results, we herein generated a truncated form devoid of Box3 in which the Flag sequence was eliminated (referred to as $N_{TAIL\Delta3}$). In addition, to directly assess the possibility that the basis for the discrepancy between our data and those of the group of Kingston in terms of binding affinity could reflect use of full-length N_{TAIL} versus N_{TAIL} peptides, respectively, we also designed and purified an N_{TAIL} construct encompassing residues 482–525 (referred to as $N_{TAIL482–525}$). We then characterized the binding reactions between XD and the various N_{TAIL} forms using ITC. The experimental design allowed us to both assess the role of Box3 and the impact of an irrelevant sequence appended downstream the primary binding site, to N_{TAIL}–XD interactions.

Results

The recombinant $N_{TAIL\Delta3}$ protein and the N_{TAIL} protein bearing a Tobacco Etch virus (TEV) protease cleavage site after residue 481, designed to allow

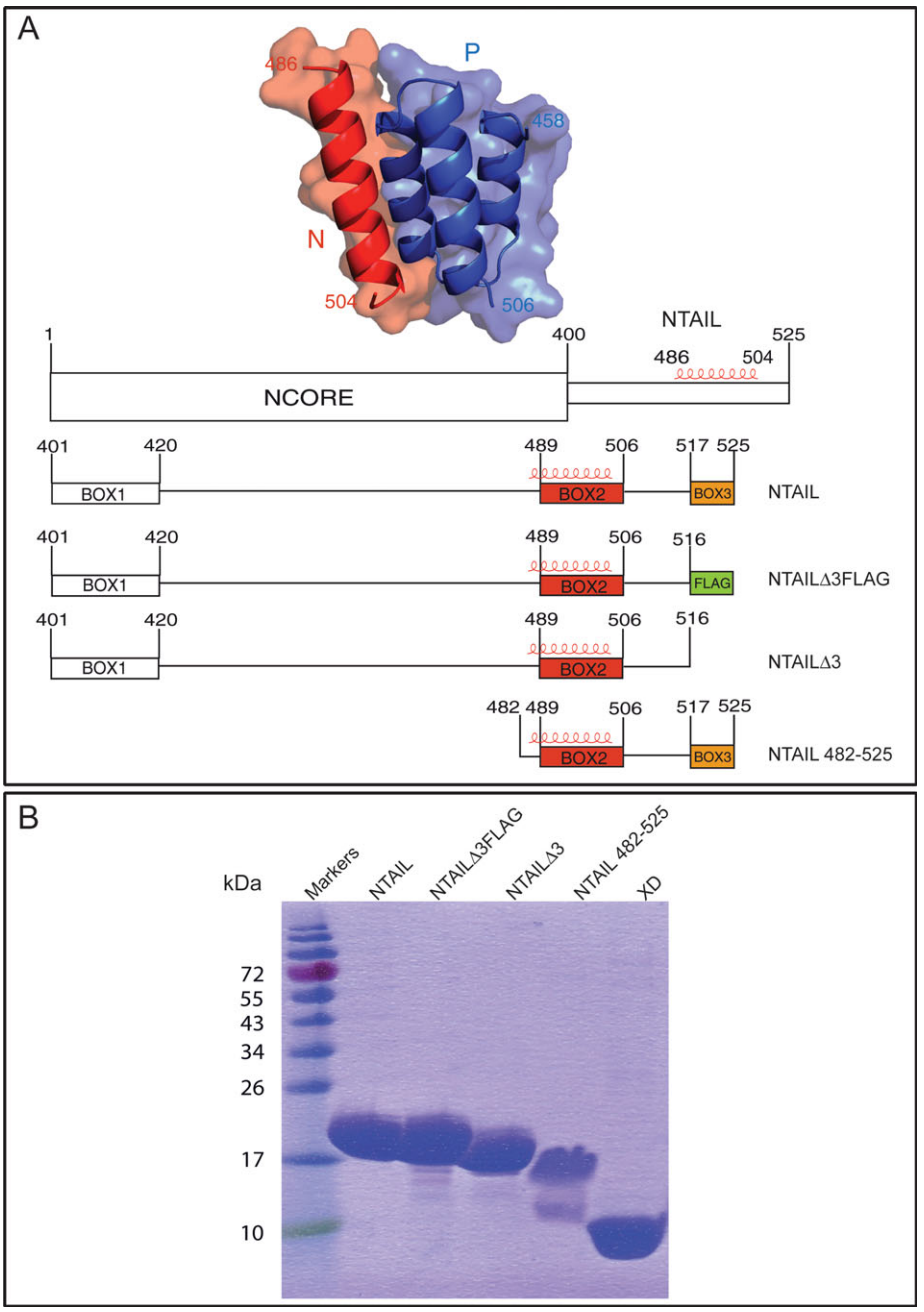

Figure 1. (A) Crystal structure of the chimera between XD (blue) and the α-MoRE of N_{TAIL} (red) (pdb code 1T6O)[21] and schematic representation of the N_{TAIL} constructs used in this study. The three conserved N_{TAIL} regions within *Morbillivirus* members are shown. Box2 and Box3 are shown in red and orange, respectively. The Flag sequence is shown as a green box. The α-helix observed in the crystal structure of the chimera is shown in red. All N_{TAIL} constructs bear an N-terminal hexahistidine tag. (B) 15% SDS-PAGE of purified proteins followed by Coomassie blue staining. [Color figure can be viewed in the online issue, which is available at wileyonlinelibrary.com.]

purification of the 482–525 region of N_{TAIL}, were all readily expressed in *E. coli* and their solubility was high, thus allowing recovery from the soluble fraction of the bacterial lysate. They were purified to homogeneity (>95%) in two steps, namely immobilized metal affinity chromatography (IMAC) and size exclusion chromatography (SEC), as was the case of the N_{TAIL} and $N_{TAILΔ3Flag}$ proteins[2] [Fig. 1(B)]. The $N_{TAILΔ3}$ and $N_{TAILΔ3Flag}$ proteins were eluted from the gel filtration S200 column with a profile quite similar to that observed for the full-length N_{TAIL} protein (data not shown), consistent with similar conformational properties.

After digestion with TEV protease of the purified N_{TAIL} protein bearing a TEV protease cleavage site, the (untagged) N_{TAIL} region encompassing residues 482–525 was recovered in the unretained fraction of an additional IMAC step. The final purified $N_{TAIL482–525}$ product consists of two bands: a major band with an apparent molecular mass of ~17 kDa,

and a minor band with an apparent molecular mass of ~12 kDa [Fig. 1(B)]. The identity of the $N_{TAIL\Delta3}$ and $N_{TAIL482–525}$ proteins was confirmed by mass spectrometry analysis of the tryptic fragments obtained after digestion of the purified proteins excised from sodium docecyl sulfate (SDS)-polyacrylamide gels, which yielded a high-sequence coverage and showed that the minor band observed in the $N_{TAIL482–525}$ sample corresponds to a degradation product (data not shown). Note that the identity of the full-length N_{TAIL} and of $N_{TAIL\Delta3Flag}$ proteins had been already confirmed in previous studies.[2,12]

All the N_{TAIL} proteins migrate in SDS-polyacrylammide gel electrophoresis (PAGE) with an apparent molecular mass higher than expected (expected molecular masses are approximately as follows: 15 kDa for full-length N_{TAIL}, 14.5 kDa for $N_{TAIL\Delta3Flag}$, 13.5 kDa for $N_{TAIL\Delta3}$, and 4.9 kDa for $N_{TAIL482–525}$), with this abnormal migration being particularly pronounced in the case of $N_{TAIL482–525}$ [Fig. 1(B)]. This peculiar migratory behavior is well documented for parental N_{TAIL}[12] and has also been reported for all N_{TAIL} variants described so far.[4,26] Such an anomalous electrophoretic mobility is frequently observed in intrinsically disordered proteins and is to be ascribed to a relatively high content in acidic residues,[28,29] and/or to a high degree of protein extension in solution.[30]

We then investigated the binding abilities of the N_{TAIL} proteins using ITC. The purified N_{TAIL} proteins were loaded into the calorimeter sample cell, and titrated with XD (Fig. 2). The data, following integration and correction for the heats of dilution, were fit with a standard model allowing for a set of independent and equivalent binding sites (Fig. 2). The K_D was derived from the K_A, as the reciprocal of this latter. The estimates for the binding parameters of N_{TAIL}, $N_{TAIL\Delta3}$, and $N_{TAIL\Delta3Flag}$ revealed a stoichiometry of ~0.7 (see Fig. 2 and Table I). Errors in the estimates of XD concentration are the most plausible explanation for this subunity stoichiometry. An even lower stoichiometry (0.52) was found in the case of the binding reaction with $N_{TAIL482–525}$ (Table I), and this may reflect inability of part of the $N_{TAIL482–525}$ sample to interact with XD, in agreement with the presence of a degradation product (possibly not competent for binding) in the purified $N_{TAIL482–525}$ sample [Fig. 1(B)].

The obtained parameters also revealed that the binding reactions are all enthalpy-driven, being all characterized by a small unfavorable entropic contribution (Table I), which is consistent with the entropic penalty associated to the disorder-to-order transition of N_{TAIL} upon binding.

The measured K_D for the binding reaction between XD and full-length N_{TAIL} is 170 ± 20 n*M* (Fig. 2 and Table I). Notably, removal of Box3 causes only a slight decrease in the affinity toward XD, with the K_D increasing twofolds but still remaining in the n*M* range (Fig. 2 and Table I). This finding argues for a minimal impact of Box3 on binding to XD. Interestingly, replacing the native Box3 region by an irrelevant Flag sequence yields a K_D close to the value observed for the full-length form (Fig. 2 and Table I). This observation supports a weak stabilizing role of the Flag sequence and suggests that amino acids downstream Box2 have a slight effect on binding, with this effect being independent of sequence. Finally, a K_D of 389 ± 24 n*M* was found for the binding reaction involving $N_{TAIL482–525}$, which corresponds to (only) a twofold increase with respect to the K_D observed with full-length N_{TAIL} (Fig. 2 and Table I). The persistence of a K_D in the nanomolar range with a short N_{TAIL} construct encompassing as few as 44 residues, rules out the possibility that the discrepancy between our previous studies[2] and those obtained by the group of Kingston[27] might arise from differences in the nature of the reactants (i.e., from the use of full-length N_{TAIL} vs. N_{TAIL} peptides).

Discussion and Conclusion

The present studies support at best only a minimal effect of Box3 on binding to XD, as illustrated by the fact that removal of Box3 leads to only a twofold increase in the K_D. These findings therefore support the data reported by Kingston[27] and are hence not compatible with the two-site binding model that we previously proposed based on SPR data.[2] A possible explanation for the discrepancy between our previous SPR data and the present ITC data may reside in possible limitations of the former approach when it comes to the analysis of very fast binding reactions such as those involving truncated N_{TAIL} forms, a point that was already raised by Kingston.[27] In light of the present ITC data, previous NMR studies showing a magnetic perturbation within Box3 associated to N_{TAIL}–XD binding,[7] as well as previous electron paramagnetic resonance (EPR) data documenting a gain of rigidity in Box3 upon binding to XD,[4] should be interpreted as reflecting only a modified Box3 environment resulting from the α-helical transition taking place in the neighboring Box2 region and not a contribution of Box3 to N_{TAIL}–XD binding.

Sequences downstream of Box2 do however contribute to N_{TAIL}–XD binding: indeed, appending an irrelevant sequence downstream of the primary binding site leads to a K_D close to that observed with full-length N_{TAIL}. This weakly stabilizing effect does not reflect entropic stabilization,[31] as the entropic penalty of the binding reaction with $N_{TAIL\Delta3Flag}$ is more pronounced than that observed with $N_{TAIL\Delta3}$. This is consistent with a scenario where Box2 is more flexible (i.e., less tightly bound to XD) in the absence of a downstream region and would explain the lower entropic penalty of

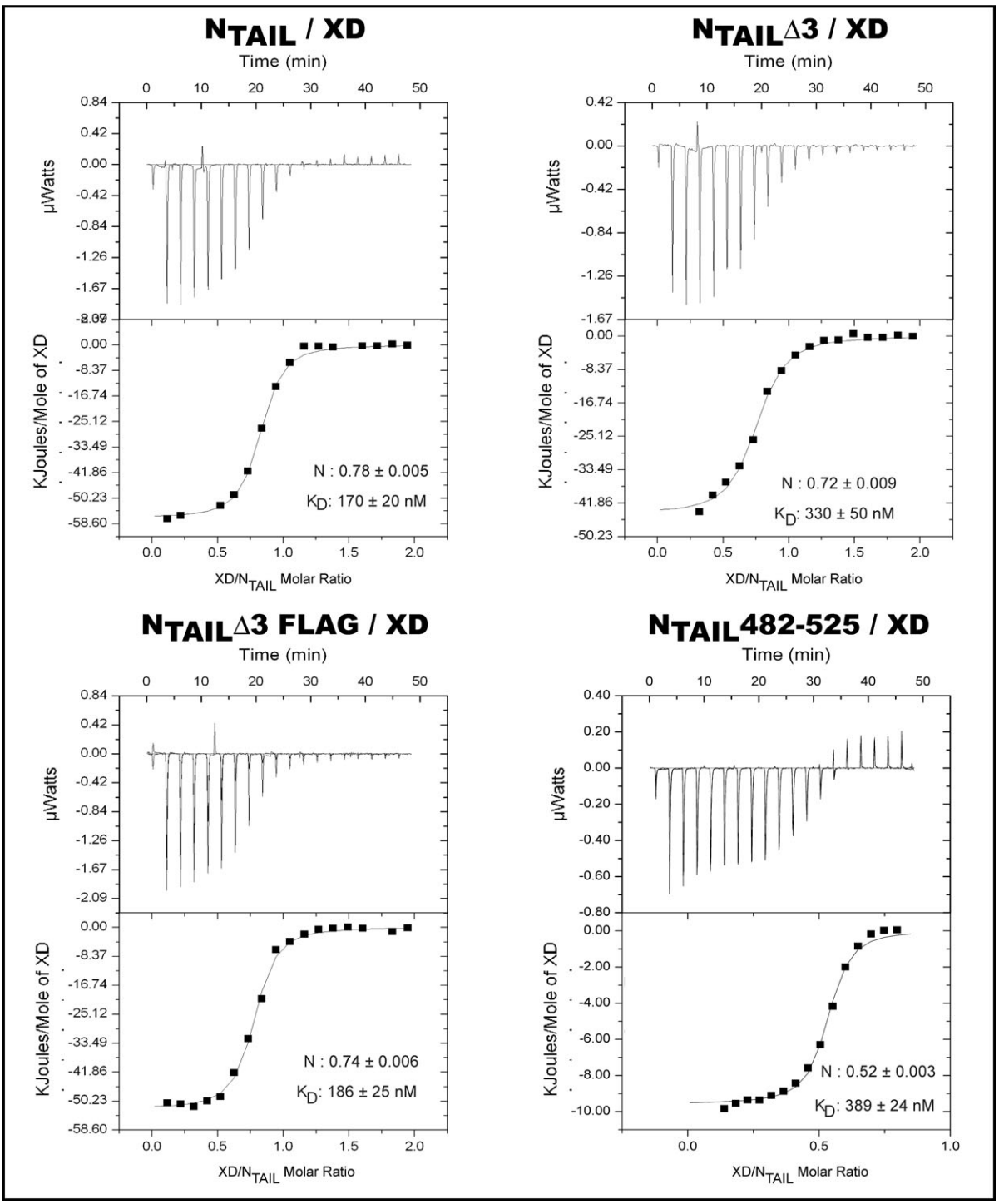

Figure 2. ITC studies of complex formation between XD and the various N_{TAIL} proteins. Data are representative of at least two independent experiments. The concentrations of N_{TAIL} proteins in the microcalorimeter cell was 20 µ*M* and that of XD in the microsyringe was 200 µ*M*. Graphs shown in the bottom of each panel correspond to integrated and corrected ITC data fit to a single set of sites model (all sites identical and equivalent). The filled squares represent the experimental data, whereas the solid line corresponds to the model. The derived equilibrium dissociation constant (K_D) as well as the stoichiometric number are shown.

$N_{TAIL\Delta3}$ as compared to both full-length N_{TAIL} and $N_{TAIL\Delta3Flag}$ (Table I).

Results of this study are consistent with previous work, in which the K_D of the N_{TAIL}–XD binding reaction is in the n*M* range.[2,26] In further support of a tight N_{TAIL}–XD complex is the relatively long half-life of active MeV P-L transcriptase complexes tethered on the nucleocapsid template, which has been determined to be well over 6 h.[32] Moreover, such a high affinity is consistent with the ability to readily

Table I. *Equilibrium Dissociation Constants and Binding Parameters, as Derived From ITC Studies, for the Binding Reactions Between MeV XD and Four MeV N_{TAIL} Proteins, namely the Full-Length Form, a Form Devoid of Box3 ($N_{TAIL\Delta3}$), a Form in Which the Native Box3 Sequence is Replaced by the Flag Sequence ($N_{TAIL\Delta3Flag}$) and a Form-Encompassing Residues 482–525 ($N_{TAIL482–525}$)*

	Stoichiometry, n	K_D (nM)	Binding enthalpy, ΔH (cal mol^{-1})	Binding entropy, ΔS (cal mol^{-1} deg^{-1})
N_{TAIL}	0.78 ± 0.005	170 ± 20	−13,537 ± 164	−14.4
$N_{TAIL\Delta3}$	0.72 ± 0.009	330 ± 50	−10,635 ± 242	−6.0
$N_{TAIL\Delta3Flag}$	0.74 ± 0.006	186 ± 25	−12,525 ± 154	−11.2
$N_{TAIL482–525}$	0.52 ± 0.003	389 ± 24	−9560 ± 125	−3.3

Data are representative of two independent trials.

purify nucleocapsid-P complexes using rather stringent techniques such as CsCl isopycnic density centrifugation.[33–36]

A tight N_{TAIL}–XD complex is not compatible with progressive movement of the viral polymerase complex along the nucleocapsid template. In fact, recent studies show that MeV polymerase activity (transcriptase elongation rate) is relatively constant over a wide range of N_{TAIL}–XD binding affinities, with this having been shown using Box2 mutations that either maintained parent N_{TAIL}–XD binding affinity or reduced this latter by as much as 30-fold.[26] That the P-N_{TAIL} binding affinity is not necessarily the primary determinant of a relatively slow polymerase elongation rate is further supported by observations in Sendai virus, where the polymerase elongation rate is even lower (i.e., 1.7 nt/s) than that of MeV (3.3 nt/s)[32] and yet the N_{TAIL}–XD complex has a K_D of 60 μM.[37] The finding that a relatively high MeV N_{TAIL}–XD binding affinity does not impose constraint on (i.e., does not slow down) viral transcriptase function[26] can be accounted for by two possible scenarios. In the first one, binding and release would not be required for transcription and replication: the P protein would be permanently bound to the nucleocapsid template and the polymerase would jump between adjacent P molecules. The so-called "jumping" mechanism has been proposed in the case of rabies virus (see Ref. [38] and references therein cited), where (i) multimerization of P was shown to be dispensable for transcription[39] and (ii) a similarly high affinity (K_D = 160 nM) between N:RNA rings and the C-terminal domain of the phosphoprotein was observed.[40] In this model, progress of the polymerase along the nucleocapsid template would rely on the dynamic breaking and reforming of contacts between L and P. The second possible scenario would rely on cellular cofactor(s) that might modulate the strength of the N_{TAIL}–XD interaction and thereby facilitate cartwheeling. The major inducible heat shock protein (hsp70) was shown to stimulate MeV transcription and replication and to compete with XD for N_{TAIL} binding.[41–44] Based on these findings, it has been proposed that the basis for the hsp70-dependent stimulation of transcription and replication would reside in the ability of hsp70 to destabilize the N_{TAIL}–XD complex, thereby promoting cycles of binding and release of the polymerase complex.[10,11]

In conclusion, the present study supports binding of one N_{TAIL} molecule per XD molecule, as already reported for the full-length N_{TAIL} protein,[2] and shows that the MeV N_{TAIL}–XD binding reaction is characterized by a submicromolar affinity. As we consistently obtained a K_D in the nanomolar range irrespective of whether we used full-length or N_{TAIL} peptides, we can rule out differences in the length of the reactants as a possible basis for the discrepancy with the data obtained by the group of Kingston.[27] We can only speculate that the presence of the nonnative TS dipeptide appended at the N-terminus of the N_{TAIL} peptides used in the ITC studies by Kingston and coworkers is a possible basis for the experimentally observed differences, thereby leading to the calculation of a K_D in the micromolar range.

Materials and Methods

Generation of N_{TAIL} constructs and purification of recombinant N_{TAIL} proteins

The coding region of the $N_{TAIL\Delta3}$ construct was obtained by polymerase chain reaction (PCR) using Phusion (Finnzymes) polymerase, the plasmid pDEST14/$N_{TAIL\text{-}HN}$, which encodes residues 401–525 of the Edmonston B MeV N protein with an N-terminal hexahistidine tag,[2] as template and a couple of mutagenic primers (Operon) designed to introduce a TAA stop codon at position 517. After digestion with *Dpn*I (New England Biolabs) to remove the methylated DNA template, CaCl2-competent *E. coli* TAM1 cells (Active Motif) were transformed with the amplified PCR product.

The $N_{TAILTEV481}$ construct, encoding residues 401–525 of the Edmonston B MeV N protein with a TEV cleavage site (ENLYFQG) inserted after residue 481 and with a hexahistidine tag fused to its N-terminus, was obtained by PCR using as template the pDEST14/N_{TAILHN} construct.[2] Forward F-1 primer was designed to amplify an N_{TAIL}-encoding fragment (fragment A) including the *AttB1* sequence, while reverse R-1 primer was designed to introduce a TEV site after the codon encoding Ser481 of N.

Concomitantly, fragment B was obtained by an independent PCR, using forward F-2 primer, designed to introduce a TEV site before codon encoding Ser482 of N, and reverse R-2 primer designed to amplify the downstream N_{TAIL} fragment including the *AttB2* sequence. Finally, a third PCR was carried out by using fragments A and B as template, and F-1 and R-2 as primers to yield the final amplification product. After purification (PCR Purification Kit, Qiagen), this latter was cloned into the pDEST14 vector (Invitrogen) using the Gateway recombination system (Invitrogen). The sequence of the coding region of all the expression plasmids was verified by sequencing (GATC Biotech) and found to conform to expectations.

The *E. coli* strains Rosetta [DE3] pLysS (Novagen) was used for expression of all recombinant proteins as already described,[1,2] except that 2YT was used instead of LB medium. The induced cells were harvested, washed, and collected by centrifugation (5000 g, 10 min). The resulting bacterial pellets were frozen at −20°C.

Purification of histidine-tagged N_{TAIL} and XD proteins was carried out as previously described,[1,2] except that in the case of XD a washing step in the presence of increasing NaCl concentrations (from 0.5 up to 2*M*) was added before elution from the IMAC column. In the case of the N_{TAIL} protein bearing a TEV protease site, the eluate from IMAC was desalted by using a HiPrep 26/10 desalting column (GE Healthcare), and the protein was eluted in buffer A (50 m*M* sodium phosphate pH 7, 300 m*M* NaCl, 10 m*M* imidazole). Cleavage with TEV protease was carried out overnight at 4°C using 1 mg of TEV per 10 mg of target protein. The TEV protease, bearing a hexahistidine tag, was purified by IMAC followed by SEC as already described[45] (data not shown). After TEV digestion, the sample was incubated 1 h with gentle shaking with 4-mL chelating sepharose fast flow resin preloaded with Ni^{2+} ions (GE Healthcare), previously equilibrated in buffer A. The flow-through was then loaded onto a Superdex 200 16/60 column (GE Healthcare) and eluted in 10 m*M* sodium phosphate pH 7. The protein was concentrated using Centricon Plus-20 (molecular cutoff: 3000 Da) (Millipore). All purified proteins were stored in 10 m*M* sodium phosphate buffer pH 7 at −20°C. All purification steps, except for gel filtrations, were carried out at 4°C. Apparent molecular mass of proteins eluted from gel filtration columns was deduced from a calibration carried out with LMW and HMW calibration kits (GE Healthcare). Protein concentrations were calculated using the theoretical absorption coefficients ε (mg mL^{-1} cm^{-1}) at 280 nm as obtained using the program ProtParam at the EXPASY server (http://www.expasy.ch/tools).

Mass spectrometry (MALDI-TOF)

The identity of the purified $N_{TAIL\Delta3}$ and $N_{TAIL482–525}$ proteins was confirmed by mass spectral analysis of tryptic fragments. The latter was obtained by digesting (0.25 μg trypsin) 1 μg of purified recombinant protein obtained after separation onto SDS-PAGE. The tryptic peptides were analyzed using an Autoflex II TOF/TOF. Spectra were acquired in the linear mode. Samples (0.7 μL containing 15 pmol) were mixed with an equal volume of sinapinic acid matrix solution, spotted on the target, then dried at room temperature for 10 min. The tryptic fragments were analyzed in the Autoflex matrix-assisted laser desorption ionization/time of flight (MALDI-TOF) (Bruker Daltonics, Bremen, Germany). Peptide fingerprints were obtained and compared with *in silico* protein digest (Biotools, Bruker Daltonics, Germany). The mass standards were either autolytic tryptic peptides or peptide standards (Bruker Daltonics).

Isothermal titration calorimetry

ITC experiments were carried out on a ITC200 isothermal titration calorimeter (Microcal, Northampton) at 20°C. In these studies, the concentration of N_{TAIL} proteins was adjusted to 20 μ*M* in the microcalorimeter cell (0.2 mL). The XD protein (stock solution at 200 μ*M*) was added from a computer-controlled 40-μL microsyringe via a total of 19 injections of 2 μL each at intervals of 150 s. Note that the same XD sample was used in all these studies. Whatever the binding reaction being studied, the pair of proteins used in each binding assay were dialyzed against a 10 m*M* sodium phosphate buffer pH 7 to minimize undesirable buffer-related effects. The dialysis buffer was used in all preliminary equilibration and washing steps.

Heat dilution of the ligand was taken into account from peaks measured after full saturation of the protein sample contained in the microcalorimeter cell by the ligand. A theoretical titration curve was fitted to the experimental data using the ORIGIN software (Microcal). This software uses the relationship between the heat generated by each injection and ΔH° (enthalpy change in cal mol^{-1}), K_A (association binding constant in M^{-1}), n (number of binding sites per monomer), total protein concentration, and free and total ligand concentrations. The variation in the entropy (ΔS in cal mol^{-1} deg^{-1}) of each binding reaction was inferred from the variation in the free energy (ΔG), where this latter was calculated from the following relation: $\Delta G = -RT$ Ln $1/K_A$.

Acknowledgments

The authors thank Christophe Flaudrops and Nicholas Armstrong from the mass spectrometry platform of the IFR48 of Marseille for mass spectrometry analyses. The funders had no role in study design, data collection and analysis, decision to publish, or preparation of the manuscript.

References

1. Johansson K, Bourhis JM, Campanacci V, Cambillau C, Canard B, Longhi S (2003) Crystal structure of the measles virus phosphoprotein domain responsible for the induced folding of the C-terminal domain of the nucleoprotein. J Biol Chem 278:44567–44573.
2. Bourhis JM, Receveur-Bréchot V, Oglesbee M, Zhang X, Buccellato M, Darbon H, Canard B, Finet S, Longhi S (2005) The intrinsically disordered C-terminal domain of the measles virus nucleoprotein interacts with the C-terminal domain of the phosphoprotein via two distinct sites and remains predominantly unfolded. Protein Sci 14:1975–1992.
3. Morin B, Bourhis JM, Belle V, Woudstra M, Carrière F, Guigliarelli B, Fournel A, Longhi S (2006) Assessing induced folding of an intrinsically disordered protein by site-directed spin-labeling EPR spectroscopy. J Phys Chem B 110:20596–20608.
4. Belle V, Rouger S, Costanzo S, Liquiere E, Strancar J, Guigliarelli B, Fournel A, Longhi S (2008) Mapping alpha-helical induced folding within the intrinsically disordered C-terminal domain of the measles virus nucleoprotein by site-directed spin-labeling EPR spectroscopy. Proteins 73:973–988.
5. Bernard C, Gely S, Bourhis JM, Morelli X, Longhi S, Darbon H (2009) Interaction between the C-terminal domains of N and P proteins of measles virus investigated by NMR. FEBS Lett 583:1084–1089.
6. Bischak CG, Longhi S, Snead DM, Costanzo S, Terrer E, Londergan CH (2010) Probing structural transitions in the intrinsically disordered C-terminal domain of the measles virus nucleoprotein by vibrational spectroscopy of cyanylated cysteines. Biophys J 99:1676–1683.
7. Gely S, Lowry DF, Bernard C, Ringkjobing-Jensen M, Blackledge M, Costanzo S, Darbon H, Daughdrill GW, Longhi S (2010) Solution structure of the C-terminal X domain of the measles virus phosphoprotein and interaction with the intrinsically disordered C-terminal domain of the nucleoprotein J Mol Recognit 23:435–447.
8. Kavalenka A, Urbancic I, Belle V, Rouger S, Costanzo S, Kure S, Fournel A, Longhi S, Guigliarelli B, Strancar J (2010) Conformational analysis of the partially disordered measles virus NTAIL-XD complex by SDSL EPR spectroscopy. Biophys J 98:1055–1064.
9. Ringkjøbing Jensen M, Communie G, Ribeiro ED, Jr, Martinez N, Desfosses A, Salmon L, Mollica L, Gabel F, Jamin M, Longhi S, Ruigrok RW, Blackledge M (2011) Intrinsic disorder in measles virus nucleocapsids. Proc Natl Acad Sci USA 108:9839–9844.
10. Longhi S (2009) Nucleocapsid structure and function. Curr Top Microbiol Immunol 329:103–128.
11. Longhi S, Oglesbee M (2010) Structural disorder within the measles virus nucleoprotein and phosphoprotein. Prot Peptide Lett 17:961–978.
12. Longhi S, Receveur-Brechot V, Karlin D, Johansson K, Darbon H, Bhella D, Yeo R, Finet S, Canard B (2003) The C-terminal domain of the measles virus nucleoprotein is intrinsically disordered and folds upon binding to the C-terminal moiety of the phosphoprotein. J Biol Chem 278:18638–18648.
13. Bourhis J, Johansson K, Receveur-Bréchot V, Oldfield CJ, Dunker AK, Canard B, Longhi S (2004) The C-terminal domain of measles virus nucleoprotein belongs to the class of intrinsically disordered proteins that fold upon binding to their physiological partner. Virus Res 99:157–167.
14. Wright PE, Dyson HJ (1999) Intrinsically unstructured proteins: re-assessing the protein structure-function paradigm. J Mol Biol 293:321–331.
15. Dunker AK, Oldfield CJ, Meng J, Romero P, Yang JY, Chen JW, Vacic V, Obradovic Z, Uversky VN (2008) The unfoldomics decade: an update on intrinsically disordered proteins. BMC Genomics 9(Suppl 2):S1.
16. Dunker AK, Silman I, Uversky VN, Sussman JL (2008) Function and structure of inherently disordered proteins. Curr Opin Struct Biol 18:756–764.
17. Turoverov KK, Kuznetsova IM, Uversky VN (2010) The protein kingdom extended: ordered and intrinsically disordered proteins, their folding, supramolecular complex formation, and aggregation. Prog Biophys Mol Biol 102:73–84.
18. Uversky VN (2010) The mysterious unfoldome: structureless, underappreciated, yet vital part of any given proteome. J Biomed Biotechnol 2010:568068.
19. Uversky VN, Dunker AK (2010) Understanding protein non-folding. Biochim Biophys Acta 1804:1231–1264.
20. Diallo A, Barrett T, Barbron M, Meyer G, Lefevre PC (1994) Cloning of the nucleocapsid protein gene of peste-des-petits-ruminants virus: relationship to other morbilliviruses. J Gen Virol 75:233–237.
21. Kingston RL, Hamel DJ, Gay LS, Dahlquist FW, Matthews BW (2004) Structural basis for the attachment of a paramyxoviral polymerase to its template. Proc Natl Acad Sci USA 101:8301–8306.
22. Oldfield CJ, Cheng Y, Cortese MS, Romero P, Uversky VN, Dunker AK (2005) Coupled folding and binding with alpha-helix-forming molecular recognition elements. Biochemistry 44:12454–12470.
23. Mohan A, Oldfield CJ, Radivojac P, Vacic V, Cortese MS, Dunker AK, Uversky VN (2006) Analysis of molecular recognition features (MoRFs). J Mol Biol 362: 1043–1059.
24. Fuxreiter M, Tompa P, Simon I (2007) Local structural disorder imparts plasticity on linear motifs. Bioinformatics 23:950–956.
25. Vacic V, Oldfield CJ, Mohan A, Radivojac P, Cortese MS, Uversky VN, Dunker AK (2007) Characterization of molecular recognition features, MoRFs, and their binding partners. J Proteome Res 6:2351–2366.
26. Shu Y, Habchi J, Costanzo S, Padilla A, Brunel J, Gerlier D, Oglesbee M, Longhi S (in press) Plasticity in structural and functional interactions between the phosphoprotein and nucleoprotein of measles virus. J Biol Chem 287:11951–11967.
27. Yegambaram K, Kingston RL (2010) The feet of the measles virus polymerase bind the viral nucleocapsid protein at a single site. Protein Sci 19:893–899.
28. Iakoucheva LM, Kimzey AL, Masselon CD, Smith RD, Dunker AK, Ackerman EJ (2001) Aberrant mobility phenomena of the DNA repair protein XPA. Protein Sci 10:1353–1362.
29. Tompa P (2002) Intrinsically unstructured proteins. Trends Biochem Sci 27:527–533.
30. Blocquel D, Habchi J, Gruet A, Blangy S, Longhi S (2012) Compaction and binding properties of the intrinsically disordered C-terminal domain of Henipavirus nucleoprotein as unveiled by deletion studies. Mol Biosyst 8:392–410.
31. Blenner MA, Shur O, Szilvay GR, Cropek DM, Banta S (2010) Calcium-induced folding of a beta roll motif requires C-terminal entropic stabilization. J Mol Biol 400:244–256.
32. Plumet S, Duprex WP, Gerlier D (2005) Dynamics of viral RNA synthesis during measles virus infection. J Virol 79:6900–6908.
33. Robbins SJ, Bussell RH (1979) Structural phosphoproteins associated with purified measles virions and cytoplasmic nucleocapsids. Intervirology 12:96–102.

34. Stallcup KC, Wechsler SL, Fields BN (1979) Purification of measles virus and characterization of subviral components. J Virol 30:166–176.
35. Robbins SJ, Bussell RH, Rapp F (1980) Isolation and partial characterization of two forms of cytoplasmic nucleocapsids from measles virus-infected cells. J Gen Virol 47:301–310.
36. Oglesbee M, Tatalick L, Rice J, Krakowka S (1989) Isolation and characterization of canine distemper virus nucleocapsid variants. J Gen Virol 70:2409–2419.
37. Houben K, Marion D, Tarbouriech N, Ruigrok RW, Blanchard L (2007) Interaction of the C-terminal domains of sendai virus N and P proteins: comparison of polymerase-nucleocapsid interactions within the paramyxovirus family. J Virol 81:6807–6816.
38. Leyrat C, Gerard FC, de Almeida Ribeiro ED, Jr, Ivanov I, Ruigrok RW, Jamin M (2010) Structural disorder in proteins of the rhabdoviridae replication complex. Protein Pept Lett 17:979–987.
39. Jacob Y, Real E, Tordo N (2001) Functional interaction map of lyssavirus phosphoprotein: identification of the minimal transcription domains. J Virol 75:9613–9622.
40. Ribeiro ED, Jr, Leyrat C, Gerard FC, Albertini AA, Falk C, Ruigrok RW, Jamin M (2009) Binding of Rabies virus polymerase cofactor to recombinant circular nucleoprotein-RNA complexes. J Mol Biol 394:558–575.
41. Zhang X, Glendening C, Linke H, Parks CL, Brooks C, Udem SA, Oglesbee M (2002) Identification and characterization of a regulatory domain on the carboxyl terminus of the measles virus nucleocapsid protein. J Virol 76:8737–8746.
42. Zhang X, Bourhis JM, Longhi S, Carsillo T, Buccellato M, Morin B, Canard B, Oglesbee M (2005) Hsp72 recognizes a P binding motif in the measles virus N protein C-terminus. Virology 337:162–174.
43. Carsillo T, Zhang X, Vasconcelos D, Niewiesk S, Oglesbee M (2006) A single codon in the nucleocapsid protein C terminus contributes to in vitro and in vivo fitness of Edmonston measles virus. J Virol 80: 2904–2912.
44. Oglesbee M. Nucleocapsid protein interactions with the major inducible 70 kDa heat shock protein. In: Longhi S, Ed. (2007) Measles virus nucleoprotein. Hauppage, NY: Nova, pp 53–98.
45. Vincentelli R, Bignon C, Gruez A, Canaan S, Sulzenbacher G, Tegoni M, Campanacci V, Cambillau C (2003) Medium-scale structural genomics: strategies for protein expression and crystallization. Acc Chem Res 36: 165–172.